

A NEW INTERPRETATION OF TIME-DEPENDENT PHYSICAL HARDENING IN ASPHALT BASED ON DSC AND OPTICAL THERMOANALYSIS

P. Claudy, J.M. Letoffe, *F. Rondelez, **L. Germanaud, ***G. King and
***J.P. Planche.

Laboratoire de Thermochimie Minérale, CNRS URA 116,
20 Avenue Albert Einstein, 69621 Villeurbanne Cedex - France

*Université Paris VI, Laboratoire de Physico-Chimie des Surfaces et
Interfaces, Institut Curie,
11, rue Pierre et Marie Curie, 75231 Paris Cedex 05 - France

**Centre de Recherche Elf,
BP22 60360 St Symphorien d'Ozon - France

***Elf Asphalt Laboratory,
400 North 10th Street, P.O. Box 1507, Terre Haute, Indiana - USA

Keywords: DSC, Asphalt Physical Hardening, Thermomicroscopy.

INTRODUCTION

As a part of their work for the Strategic Highway Research Program (SHRP), Anderson and Bahia recently reported an important phenomenon in asphalt cement they defined as "low temperature physical hardening" (1,2,3). This effect seems to be caused by a gradual density change that occurs over time when bitumens are held at low temperatures. The mechanical stiffness of the asphalt increases markedly in response to this decrease in volume. They were able to demonstrate that the changing stiffness can be explained by time-dependent shift factors not unlike those used to explain time-temperature superposition in conventional rheological measurements.

In other recent papers (4,5,6,7), Claudy and coworkers used Differential Scanning Calorimetry (DSC) and two thermomicroscopy methods (polarized light and phase contrast) to identify certain molecular associations within asphalt defined as "crystallized fractions". The associating species are more prevalent in the saturates fraction of the bitumen, and thus are thought to be highly aliphatic molecules. Even though Crystallized fractions are more evident at low temperatures, they begin to form at temperatures as high as 80°C, and then continue to precipitate as the asphalt cools.

This study was designed to characterize the temperature and time dependent structural changes that occur in the eight SHRP core asphalts. There are two important questions to be answered: "Are the newly observed phases truly crystalline?" and "Does the formation of multiple phases at low temperatures contribute to the low temperature isothermal

hardening of asphalt cement. It is not unreasonable to predict volume shrinkage should occur upon phase separation if the associating molecules occupy less volume than they did in a homogeneous liquid state. If this process occurs at the same temperatures and over the same time scales used in Anderson's experiments, then it should be possible to gain some insight regarding the physico-chemical changes which contribute to physical hardening. The first step is to relate the structuring observed by DSC and thermomicroscopy to the time-dependent changes in the rheological properties of the asphalt cement.

Then, the underlying chemical interactions which cause the observed structural changes will be characterized. Since previous DSC studies have demonstrated that the thermal effects are most evident in the saturates fraction, it seems most probable that weak Van der Waals forces are causing aggregation of the aliphatic chains, creating localized regions with a density and refractive index different from that of the bulk asphalt. These aliphatic species may be n-alkanes (waxes), or they may be long side chains on much larger molecules. As was discussed in some detail elsewhere (8), n-alkanes from C-10 to C-20 melt within the temperature range of -30 to 40 °C, which corresponds to pavement service temperatures. However, adding a double bond anywhere in the alkyl chain will typically reduce the melting temperature by 30 to 90°C. Placing the aliphatic chain in a sterically hindered environment, such as on an aromatic or aliphatic cyclic system, will also reduce its tendency to agglomerate with other molecules. To confirm that aliphatic species are indeed responsible for the enthalpy changes observed by DSC and the localized refractive index differences observed by microscopy, model asphalts have been formed by adding pure n-alkanes (n = 20 to 40) to selected asphalts.

Finally, we have attempted to describe how the physico-chemical changes occur. A mathematical analysis of the microscopic images was used to evaluate the polyphasic structure within the cooled asphalt and to identify the mechanism through which the phase changes occur.

EXPERIMENTAL

In order to relate the thermal properties to the observed rheological changes, the eight SHRP core asphalts were analyzed by DSC and two thermomicroscopy techniques as reported in previous papers and summarized below. SHRP asphalt AAO and a waxy Chinese crude residue (#12) that cannot meet current bitumen specifications were also evaluated. The chemical composition of each asphalt was analyzed using IATROSCAN (a thin layer chromatography technique) to separate the nC7 maltenes into aromatic, polar, and saturates fractions (see Table 1a). The traditional physical properties of these asphalts were determined previously in ref. 7 (see also Table 1a).

The Chinese bitumen was evaluated for low temperature physical hardening by conditioning and testing samples at -15°C over a four day period. Anderson and Bahia's protocol was used to measure the creep response of conditioned samples in the Cannon Bending Beam Rheometer (BBR) (2,3). DSC experiments were carried out using a Mettler TA 2000 B apparatus controlled by a computer. The experimental procedure for the calibration of temperature and enthalpy has been previously described (9). A DSC run typically sweeps a temperature range of -100 to $+100^{\circ}\text{C}$ at a heating rate of $5^{\circ}\text{C}/\text{min}$ while the sample is maintained under an argon atmosphere. The amount of crystallized fraction (CF) was determined using a quantitative method previously described (4). Most of the detailed sample conditioning and test procedures used to obtain the DSC results presented herein have also been described elsewhere (7).

To study the effect of aliphatic compounds on thermal behavior, up to 7% pure n-alkanes ($n = 20$ to 40) were added to selected asphalts. The alkanes were supplied by Aldrich at 99+ % purity. The resulting blends were stirred for 24 hours at 100°C to guarantee homogeneity. After storing the samples another 24 hours at room temperature, DSC sweeps were run following the conventional procedure. First the samples are cooled at a rate of $10^{\circ}\text{C}/\text{min}$ to -100°C , and then thermal effects were monitored while heating the sample to 100°C at $5^{\circ}\text{C}/\text{min}$.

Optical microscopy can provide information regarding the internal structure of materials, including phenomena such as crystallization or phase separation. Binders were analyzed using equipment and experimental procedures previously described (6).

- Polarized light microscopy

This technique is most commonly employed to observe anisotropic behavior within substances which exhibit more than one refractive index, e.g. birefringent materials. Small crystallized regions within the sample may appear white or colored under polarized light. Amorphous materials such as polymers or glasses are isotropic and will not affect the light passing through them.

- Phase contrast microscopy (Zernike method)

This method is primarily applied to increase the contrast of unstained specimens when the refractive index within a region of interest is very close to that of the surrounding matrix. This device transforms differences in refractive indices into variable intensities of transmitted light.

By combining these two methods, one can observe both well-crystallized domains (polarized light) and amorphous fractions (phase contrast) contained in a glassy matrix.

THERMAL BEHAVIOR OF SHRP CORE ASPHALTS

The thermal behavior of each of the eight SHRP core asphalts was characterized using a previously described DSC procedure (7) (Figure 1). Several important features can be observed on each thermogram:

- In a narrow temperature range usually falling below 0°C, there is a clearly defined increase in heat capacity corresponding to the glass transition within the hydrocarbon matrix. The glass transition temperature (T_g) is assumed to be the midpoint of this temperature range. The corresponding change in heat capacity around T_g is designated DC_p.
- In the temperature range above 0°C, there are two or three peaks which represent changes in enthalpy within the hydrocarbon matrix. These endothermic effects are attributed to a change of state related to the dissolution of fractions that had previously been precipitated upon cooling. The term CF (crystallized fraction) designates the relative amount of material which ultimately participates in this solid-to-liquid phase change over the entire test temperature range. It is calculated by integrating the enthalpy changes measured in a DSC sweep. It is now obvious that not all of these enthalpy changes are due to formation of purely crystalline materials. Thermal parameters for the tested asphalts are listed in Table 1a.

Four asphalts (AAG, AAO, AAM, #12) were selected specifically to provide samples with a broad range of dissociating materials. They were annealed at a temperature of -15°C for periods ranging from 1 to 8 days to determine the effect of storage time on the thermal events observable by DSC. Experimental curves for AAG and AAM are shown in Figure 2, and CF results for the four asphalts are listed in Table 2a. Since AAG has a very low CF, there are no drastic changes in either CF or T_g after annealing at -15°C. On the other hand, both AAO and AAM contained over 4% CF initially, and each exhibits very significant changes in thermal properties after conditioning. During the first 24 hours at -15°C, there is a 20-40% increase in CF accompanied by a 5-10°C increase in T_g. During the following seven days, the CF remains approximately constant, but the structure within the disassociating phases appears to change markedly. Over time, the low temperature thermal effect splits into two clearly defined peaks, with the peak near 0°C appearing to grow at least partially at the expense of the peak located near 30°C. The glass transition appears to shift until it almost becomes an extension passing below the baseline of this first endothermic peak. Given the experimental precision of ±5%, precipitation seems to be essentially complete within 24 hours. However, the continuing evolution in the DSC profile, particularly in the region near 0°C, proves that the orientation of molecules within the dissociated phases changes with time. Eight days or more may be required for the system to reach equilibrium at -15°C. It is hypothesized that shorter or highly substituted alkyl chains ultimately form a structure at thermodynamic equilibrium which

dissolves very easily at low temperatures. However, upon more rapid cooling, these molecules may temporarily precipitate with larger paraffins to form one single peak, rather than the two peaks observed upon extended storage. Further doping experiments with C24 in AAG should resolve some of these questions, but these data are not yet available.

In a previous study the SHRP core asphalts were preconditioned for 24 hours at storage temperatures varied in 5°C increments from -30°C to 25°C. Results of CF versus storage temperature are shown in table 2b (7). Very little CF was detected in AAG and AAA. Generally, for the other seven asphalts, there was a gradual increase in the amount of CF as the storage temperature decreased from +25°C down to -15°C. This is fairly consistent with the theory that CF results from the precipitation of aliphatic molecules. As the temperature decreases, additional precipitation would be expected as shorter alkyl chains phase separate. However, as the storage temperature continues to drop from -15 to -30°C, the CF begins to decrease, rather than increasing as expected. Molecular motion at these very low temperatures is probably so slow that 24 hours is not sufficient for complete precipitation to occur. It is also conceivable that the mixture can supercool in such a way that some of the available molecules will not separate from solution. Further study is needed here.

TIME-DEPENDENT CHANGES IN PHYSICAL PROPERTIES

As reported previously (7), penetrations of three bitumens with moderate to high amounts of CF were reduced by 15 to 40% after only one day of storage at 5°C, even though all conditioned samples were reheated to 25°C for two hours before testing. The greatest time-dependent hardening was observed in those asphalts with higher amounts of CF as determined by DSC (see Tables 1a and 1b). These results do suggest that most of the observed penetration change occurs within the first day of storage. This is apparently not consistent with DSC observations which show that structure may continue to form for days. This inconsistency can, however, be easily explained by recalling that the pen tins are reheated to 25°C before testing. DSC curves show that much of the structure (probably shorter or highly substituted aliphatic chains) which forms over time will dissolve between T_g and 25°C. Hence, consistency measurements must be made over appropriate time intervals at the storage temperature if physical hardening effects are to be correctly evaluated.

It is worth emphasizing the importance of physical hardening by comparing it to age hardening, the oxidation-induced irreversible structural changes that occur during the hot-mix operation or in the pavement. A hardening index can be defined by the ratio of the pen after 1 day storage at -15°C vs original pen. Table 1b compares this hardening index to traditional pen aging indices. Even when the samples are reheated to 25°C for testing, the

physical hardening index suggests changes in consistency almost on the same order as the aging indices observed after the RTFO test. Unlike penetration or other physical consistency measurements made at lower temperatures, the ring and ball softening point remains relatively stable, regardless of the storage time and temperature prior to its determination (see Table 1b) (7). This result is consistent with DSC observations that enthalpy changes detectable above the softening point are fairly small. More importantly, this high temperature portion of the DSC curve is not significantly changed by storage conditions, probably because only very large aliphatic molecules that associate quickly remain agglomerated at high temperatures. This offers additional proof that the time-dependent hardening due to CF is thermoreversible.

Anderson's bending beam rheometer is an excellent tool for evaluating low temperature physical hardening, because it can provide accurate stiffness measurements at the prescribed conditioning temperature. It is also very easy to store and evaluate many samples at the test temperature without tying up the instrument or sample molds for long periods of time. But most importantly, it is possible to reduce all of the data to a single hardening shift factor, much like the shift factor derived for time-temperature superposition. The Anderson-Bahia protocol (2) was used to monitor the change in creep response of the highly paraffinic Chinese residue (#12) over 96 hours at -15°C. As shown on Figure 3, the creep compliance decreased significantly with time in storage. The hardening shift factor between 2 and 24 hours of isothermal aging is shown on Table 1b along with Anderson's data for the eight core asphalts. As expected, the shift factor for the waxy Chinese asphalt is somewhat higher.

RELATING PHYSICO-CHEMICAL CHANGES TO PHYSICAL HARDENING

Anderson reports that the hardening phenomenon, and its corresponding shift factor, is related to a measurable time-dependent volume decrease in the asphalt sample. This is probably a consequence of CF precipitation. The dominant mechanism which explains low temperature physical hardening is the formation of a new structure within the asphalt cement as phase separation occurs.

Before trying to develop any rigorous models relating chemical functionality to physical properties, it is worthwhile to review relevant data from two papers presented recently at the Rome Bitumen Chemistry Conference (2) (7). Since AAM shows the greatest physical hardening and highest CF content of the SHRP core asphalts, both Anderson and Claudy focused strongly on the evolution of this bitumen with time and temperature. First, one can visually compare the changes in the hardening shift factor of AAM as determined on the BBR (Figure 4) to the evolving endothermal effects observed by DSC after annealing at various temperatures for 24 hours

(Figure 5). As the annealing temperature decreases below -15°C , there is a gradual evolution to a third distinct endothermal effect centered around 0°C . This is consistent with the observation that lower molecular weight alkyl chains are able to precipitate upon annealing at lower temperatures. However it is also possible that a third type of structure forms at these very low temperatures which has a dissolution range lower than the other two thermal effects.

If one wants to establish a relationship between chemical and physical properties, the most obvious approach is to compare the hardening shift factor to the enthalpy changes observed by DSC. In Figure 6, CF is plotted against the hardening shift factor for the SHRP core asphalts. All samples were conditioned at -15°C for 24 hours. This simple approach resulted in a surprisingly good correlation coefficient of 0.79.

However, the hardening shift factor is not just affected by the amount of crystallizable material. When conditioning temperatures approach the glass transition range, the mobility of the molecules is greatly reduced, and the phase change occurs more slowly. Hence, some correction for molecular mobility should better explain the rate of hardening. One approach that provided a surprisingly good result for the eight core asphalts was to divide CF by the temperature difference between the conditioning/test temperature (T_c) and the glass transition temperature (T_g) as determined by DSC. When the hardening shift factor was plotted against the new parameter $CF/(T_c - T_g)$ for samples conditioned for 24 hours at -15°C , the correlation improved to $r^2 = 0.96$ (Figure 7). This suggests that asphalts harden faster when they contain more CF and when their T_g is lower (i.e. There is more molecular mobility at the conditioning temperature because the solvent phase is further from its glassy state). This represents a quite distinct difference from Anderson's interpretation, which relates the physical hardening to T_g . What is really important is the amount of crystallized fraction at the time of the measurement. Moreover, physical hardening occurs before T_g .

Even though the Chinese residue is an extreme case with a very high CF, it falls almost exactly on the line extrapolated from the SHRP asphalts. However, one must still be careful not to attach too much physical significance to the term $CF/(T_c - T_g)$, because the denominator goes to zero and is therefore undefined at $T_c = T_g$. It would be preferable to relate molecular mobility to the rheology of the total bitumen or the neutral fraction at T_c . In addition, CF represents the entire crystallized fraction, not just the additional molecular reorientation that takes place over time at the conditioning temperature. It was unfortunately not possible to accurately quantify the change in CF with time, a property which would logically reflect rates of hardening better than the total CF.

Other time-dependent parameters identified by Anderson include the early hardening rate parameter and the limiting hardening parameter. Correlations between these two parameters vs $CF/(T_c - T_g)$ were 0.93 and 0.74 resp..

Anderson also showed there is a very good correlation between physical hardening and a time dependent decrease in free volume. This, too, is consistent with DSC observations. As aliphatic molecules associate through weak Van der Waals forces, the long chains become immobile with respect to their immediate neighbors, and hence occupy less free volume. Therefore if the formation of CF is time dependent, there should be a corresponding decrease in volume as the process occurs.

ADDITION OF N-ALKANES

The excellent correlation between DSC and physical hardening immediately raises another question, "What chemical functionalities precipitate out of solution at low temperatures." A partial response was given by Claudy et al. (3) when they showed that only the saturate fractions from a SARA separation exhibit strong endothermal effects corresponding to a dissolution process. None of the other three fractions (aromatics, polar aromatics or asphaltenes) exhibit significant enthalpy changes above T_g , leading to the assumption that most of the agglomerating molecules come from the saturate fraction. Hence, the next logical step was to dope bitumens with various pure n-alkanes and then analyze the thermal behavior of each mixture.

First, six pure n-alkanes (C20, C24, C28, C32, C36, C40) were analyzed by DSC using the reference procedure cited above. The corresponding thermograms are compared on Figure 8. C20 and C40 each have one single peak, whereas the other four alkanes each show two different peaks, one related to a solid-solid transition and the other to melting.

In a second experiment, 3% of each alkane was added to asphalt AAG, which contains virtually no CF. The resulting thermal parameters are listed in Table 3, while Figure 9 shows the differential DSC thermograms of the doped AAG samples for each of the six alkanes. Several observations are notable:

- Both the pure n-alkanes and the doped asphalts exhibit increasingly higher melting and dissolution temperatures respectively as the molecular weight of the alkane increases.
- The dissolution temperature range of the alkane is much broader when it is dissolved in the bitumen.
- When dispersed in the asphalt, the n-alkane begins to dissolve at a temperature which is typically 20-30°C below its pure melting point. This suggests strong interactions between the paraffins and the asphalt matrix.
- Upon heating, the total enthalpy required to dissolve the alkane back into the asphalt is surprisingly close to the enthalpy of melting for the pure n-alkane,
- For C20, C32, C36, C40 only one endothermal peak is seen.

Observations of the data (Table 3) indicate that T_g is systematically lowered upon addition of paraffins, 18°C for C20, 9°C for C24, 4°C for C28.

In another doping experiment, 1 to 6% of C24 paraffin was added to asphalt AAG. DSC fingerprints are presented on Figure 10, and thermal parameters are included on Table 3. Two peaks are generally observed, but the relative area under each changes dramatically with concentration of paraffin. At the lowest concentration of 1.06%, the thermal effect above 35°C is very broad and no second peak is evident. Above 2% C24, the first peak between 0 and 35°C seems to reach a saturation point, and most of the enthalpy change resulting from continued addition of paraffin appears in the second peak above 35°C. This represents a dramatic difference in dissolution temperatures, implying there must be formation of two liquids within the solvent phase. Perhaps not coincidentally, virgin asphalts with significant amounts of CF also show two peaks with a minimum at 35°C. Hence one would like to postulate that paraffins cause asphalt to separate into two distinct liquid phases. This might explain the two different sized domains as observed by Phase Contrast (1-3 microns) and Polarized Light (10-15 microns) microscopy. Verney et al reported that there seems to be a natural transition in rheological properties around 35°C. This effect is so important that they propose two different rheological models to fit data above and below this temperature (10).

The same general trends were observed when 1 to 5% C24 was added to AAM, the SHRP core asphalt with the highest natural CF. Differential DSC curves, which subtract the pure bitumen curves from doped asphalt thermograms, clearly show two peaks splitting at 35°C (see Figure 11). However, since AAM already contains a large amount of CF, the second peak is much more strongly affected by the first percent of added paraffin. Apparently, there is already enough natural paraffin present in AAM to interact with one liquid phase. Therefore, most of the added C24 separates on cooling into a different type of structure, hypothesized to be a more crystalline waxlike solid which dissolves at higher temperatures.

When Claudy et al compared the thermal behavior of asphalt to that of other petroleum fractions (kerosene, diesel oil, crude oil) some curious anomalies were discovered (7). Even though all of these products exhibit aliphatic crystallization at low temperatures, only asphalt displays more than one endothermal peak in the dissolution range, and only asphalt exhibits time-dependent structural changes. The time-dependence might be explained by recognizing that the viscosity within the asphalt matrix at these temperatures is very high, so the mobility of molecules is greatly reduced. The two peaks observed may represent the following phenomenon:

- Below T_g , the precipitated paraffins are dispersed within the solid glassy matrix.

- Immediately above T_g , the liquid continuous phase (L) still contains organized paraffinic entities (P). As the solid paraffins begin to dissolve upon heating, the combined liquid (L+P) immediately begins to separate into two different liquid phases, (L' + P) and (L''). This process, which is responsible for the first peak, essentially continues until the solid paraffins are dissolved,

or until the portion of the solvent phase most compatible with the paraffins (L') is consumed.

- Assuming excess paraffin exists, then the remainder of (P) must dissolve in (L") to form (L" + P). Since this second liquid phase is much less compatible with alkanes, the paraffins cannot dissolve until the temperature becomes fairly high (>35°C). This explains the appearance of the second peak. Such behavior is well-known in other systems. For example, during polymerization, the polymer chain in formation begins to separate from the monomer phase and then dissolves in the solvent. Similar biphasic structure is also evident when some polymers are dissolved in asphalt. This hypothesis for two liquid phases is strongly supported by doping experiments in which a single pure n-alkane gives two clearly defined endothermal peaks .

Phase Contrast and Polarized Light Microscopy techniques were used to study asphalt AAG before and after doping with n-paraffins. Resulting photographs are presented in Figure 12:

- virgin AAG, which contains virtually no CF, appears to be perfectly homogeneous. There is no observable phase separation detectable by either of the two optical techniques.

- the addition of 7% C24 results in the formation of crystalline regions which are easily detected by polarized light. A definite biphasic structure is also apparent in the phase contrast photomicrograph.

- the addition of 15% n-paraffin emphasizes the phase separation and increases the crystallization phenomenon.

For comparison, photomicrographs of a vacuum distillation residue containing 14.6% natural CF are included on the same figure. The Polarized Light photos for AAG doped with 15% n-alkane and the asphalt with high CF show that the crystallized fractions are very similar in size and quantity. Phase Contrast photomicrographs also show very clear biphasic characteristics in both samples. Hence it is possible to approximately duplicate both the microscopic images and the DSC thermal effects of bitumens containing significant amounts of CF by doping asphalt AAG with n-alkanes, even though virgin AAG exhibits none of these properties.

Microscopy image statistical analysis

Microscopic images such as shown in Figure 12 were systematically analyzed by performing a two-dimensional Fourier transform. This mathematical method determines characteristic lengths of any heterogeneous regions located on the image. When phase separation within a bitumen was observed on the photomicrographs, the dissociating molecules initially formed domains of fairly uniform size, with a length of about 4 microns. Therefore, it appears that, although the final images seem to show isolated domains corresponding to crystalline fractions, the phase separation process may actually be more accurately described as a spinodal

decomposition phenomenon (11, 12). There is a periodic modulation of the concentration of paraffin within the asphalt matrix. More experiments are in progress to test this hypothesis which would, if confirmed, provide an important clue to understanding physical hardening at low temperature. The asphalt is no longer homogeneous in density. Instead, it appears to be a complex two phase structure, more akin to a gel, with enhanced viscoelastic properties.

CONCLUSION

There now seems to be no doubt that the molecular agglomerations observed by DSC and thermomicroscopy are at least partially responsible for the time-dependent shrinkage and resulting stiffening observed during low temperature isothermal aging. Ultimately, at any given temperature, the system will reach thermodynamic equilibrium, after which no additional hardening takes place. The amount of stiffening that does occur over time can be related to the number of molecules in the bitumen which coalesce to form microscopic crystalline or amorphous domains within the solvent phase. The rate at which hardening occurs is also affected by molecular mobility within the solvent phase. By correcting the total enthalpy change observed by DSC (CF) by an empirical mobility factor ($T_c - T_g$) relating the test temperature to T_g , it was possible to predict hardening shift factors with correlation coefficients of 0.96, which is quite remarkable for any chemical-physical relationships in bitumen.

Pure n-alkanes have been added to various asphalts and the resulting blends analyzed by DSC, Phase Contrast Microscopy, and Polarized Light Microscopy. It seems evident from these results that molecules containing long aliphatic chains are responsible for time-dependent structural changes. Using microscopy, one observes well-organized crystallized regions of 10-15 microns, as well as poorly-organized, amorphous domains 1-3 microns wide. Thus, asphalt microstructure is heterogeneous at low temperatures, with tiny paraffinic crystals and polar-associated molecular chains all dispersed within the solvent matrix.

One possible process for the phase separation of a single homogeneous liquid into two liquid phases upon cooling is called spinodal decomposition. It can be found in a wide variety of materials such as glasses, polymers or metals. Spinodal decomposition within asphalt was verified and quantified by applying statistical image analysis techniques to the photomicrographs. Amphoterics, or highly polar molecules, have been shown to play a key role in performance-related asphalt rheology by increasing stiffness within the liquid matrix at high temperatures. Correspondingly, the understanding of aliphatic interactions may prove to be equally enlightening regarding the tendency for pavements to thermally crack in cold environments.

REFERENCES

1. Anderson, D.A. and Christensen, D.W., 65th Annual Meeting of AAPT, Seattle, Wash., March 4-6 (1991).
2. Bahia, H.U., Anderson, D.A., International Symposium on Chemistry of Bitumens, Rome, Italy, Proceedings, 1, 114-147, June 5-8 (1991).
3. Bahia, H.U., Anderson, D.A., and Christensen, D.W., 66th Annual Meeting of AAPT, Charleston, S.Carolina, February 24-26 (1992).
4. Brûlé, B., Planche J.P., King, G.N., Claudy, P. and Letoffe, J.M., A.C.S. Symposium on Chemistry and Characterization of Asphalts, Washington, D.C., August 26-31 (1990).
5. Brûlé, B., Planche J.P., King, G.N., Claudy, P. and Letoffe, J.M., Fuel Science and Technology International, 9(1), 71-91, (1991).
6. Claudy, P., Letoffe, J.M., King, G.N. and Planche J.P., Fuel Science and Technology International, 10(4-6), 735-765, (1992).
7. Claudy, P. and Letoffe, J.M., King, G.N. and Planche J.P., International Symposium on Chemistry of Bitumens, Rome, Italy, Proceedings, 2, 530-567, June 5-8 (1991).
8. King, G.N., International Symposium on Chemistry of Bitumens, Rome, Italy, Proceedings, 2, 742-769, June 5-8 (1991).
9. Bosselet, F., Thesis No 8, St Etienne, France (1984).
10. Verney, V., Michel, A., Planche, J.P., and Brûlé, B., 25eme Colloque du Groupe Français de Rhéologie, Session 4, Rhéologie des Bitumes et Bétons Bitumineux, Grenoble, France, November 28-30 (1990).
11. Binder, K., Material Science and Technology, 5, ed. by VCH Verlagsgesellschaft Weinheim, (1991).
12. Cahn, J.W., trans. Metallurgical Soc. of AIME, 242, 166-179, (1968).

Table 1a. Physical and Chemical Properties of Study Asphalts

| Asphalt Cements | AAA | AAB | AAC | AAD | AAF | AAG | AAK | AAM | AAO | #12 |
|------------------------|-------|-------|-------|-------|-------|-------|-------|-------|-------|------|
| Saturates, wt% | 6 | 7.2 | 9.7 | 4.4 | 5.9 | 4.6 | 3.6 | 6.6 | 4.2 | 8.2 |
| Aromatics, wt% | 69.1 | 64 | 67.6 | 61.9 | 70.8 | 70.5 | 61.5 | 67.4 | 70.9 | 50.9 |
| Polar Aromatics, wt% | 13.4 | 15.1 | 10.6 | 18.7 | 14 | 21.6 | 22.9 | 23.3 | 12.5 | 28.5 |
| nC7 Asphaltenes, wt% | 11.5 | 13.7 | 12.1 | 15 | 9.3 | 3.3 | 12 | 2.7 | 12.4 | 11.7 |
| Tg, °C | -29 | -30.9 | -26.5 | -29.4 | -26.1 | -11.1 | -24.8 | -25.3 | -31.5 | -30. |
| DCp, J/g/K | 0.267 | 0.225 | 0.235 | 0.297 | 0.189 | 0.337 | 0.25 | 0.222 | 0.164 | 0.15 |
| CF, wt% | 0.4 | 4.6 | 4.9 | 1.6 | 3.7 | 0.2 | 1.2 | 5.3 | 4.4 | 10.1 |
| Penetration, 25°C, dmm | 155 | 90 | 102 | 137 | 54 | 55 | 65 | 63 | 105 | 119 |
| Ring & Ball, °C | 40.1 | 45.2 | 45 | 44 | 49.2 | 48 | 50.1 | 48.1 | 45.2 | 44.9 |
| Viscosity, 60°C, P | 640 | 920 | 670 | 880 | 1360 | 1450 | 2550 | 1690 | 960 | 326 |
| Viscosity, 135°C, cSt | 263 | 240 | 195 | 292 | 306 | 217 | 500 | 453 | 317 | 194 |
| Fraass Point, °C | -20 | -16 | -16 | -18 | -9 | -5 | -8 | -17 | -18 | -17 |

Saturates, Aromatics, Polar Aromatics determined with IATROSCAN.

Tg (Glass Transition Temperature), DCp (Heat Capacity variation), and CF (crystallized fraction) measured with DSC Values from Claudy et al.1991.

Table 1b. Physical Properties of Study Asphalts after Aging

| Asphalt Cements | AAA | AAB | AAC | AAD | AAF | AAG | AAK | AAM | AAO | #12 |
|-----------------------|-------|-------|-------|-------|------|-------|-------|-------|------|------|
| Ring & Ball*, °C | - | - | - | - | 48.3 | - | - | 49.5 | - | 45.7 |
| Penetration Ratio1, % | 51.6 | 62.2 | 52.9 | 43.8 | 53.7 | 63.6 | 61.5 | 66.7 | 59.6 | 63 |
| Penetration Ratio2, % | - | - | - | - | 88.9 | - | - | 85.7 | - | 69.7 |
| HSF, log(sec) | 0.175 | 0.325 | 0.456 | 0.225 | 0.5 | 0.106 | 0.281 | 0.612 | - | 0.64 |

*Ring & Ball after 24 hour storage at -15°C. Values from Claudy et al.1991.

Ratio1: Ratio of 25°C Penetration ratio after and before RTFO

Ratio2: Ratio of 25°C Penetration after and before 3 day storage at -15°C

HSF: Hardening Shift Factor after 24 hour isothermal age at -15°C, measured with the Benbing Beam Rheometer. SHRP asphalt HSF are from Bahia et al.1991.

Table 2a. Isothermal Age* Influence on Crystallized Fraction and Tg (-15°C)

| AC's | AAA | AAB | AAC | AAD | AAF | AAG | AAK | AAM | AAO | #12 |
|---------|-----|-----|-----|-----|-----|-------|-----|-------|-------|------|
| CF, wt% | 0 | - | - | - | - | 0.2 | - | 5.3 | 4.2 | 9.3 |
| | 1 | - | - | - | - | 0.2 | - | 7.4 | 5.5 | 13 |
| | 2 | - | - | - | - | 0.1 | - | 7.4 | 5 | 13.1 |
| | 4 | - | - | - | - | 0.1 | - | 7.5 | 5.2 | 13.2 |
| | 8 | - | - | - | - | 0.2 | - | 7.5 | 5.5 | 13 |
| Tg, °C | 0 | - | - | - | - | -11.1 | - | -28.6 | -25.3 | nm** |
| | 1 | - | - | - | - | -10 | - | -24.2 | -15.3 | nm |
| | 2 | - | - | - | - | -8.9 | - | -20.5 | -15.1 | nm |
| | 4 | - | - | - | - | -6.4 | - | -23 | -21.4 | nm |
| | 8 | - | - | - | - | -6.4 | - | -18 | -17.6 | nm |

* Isothermal Age (days) - ** not measurable - Values from Claudy et al.1991.

Table 2b. Storage Temperature Influence on Crystallized Fraction (24 hrs)

| AC's | AAA | AAB | AAC | AAD | AAF | AAG | AAK | AAM | AAO | #12 |
|---------------|-----|-----|-----|-----|-----|-----|-----|-----|-----|------|
| CF, wt% +25°C | 0.4 | 4.6 | 4.9 | 1.6 | 3.7 | 0.2 | 1.2 | 5.3 | 4.2 | 9.3 |
| +20°C | - | 4.6 | 5 | 1.4 | 3.4 | - | 1.2 | 5.7 | 4.3 | 11.5 |
| +15°C | - | 3.8 | 4.5 | 1 | 2.9 | - | 1.4 | 5.1 | 3.1 | 11.2 |
| +10°C | - | 4.2 | 4.1 | 1.7 | 3.2 | - | 1.1 | 5.2 | 2.5 | 11.4 |
| +5°C | - | 4.3 | 4.5 | 1.3 | 3.9 | - | 1.4 | 4.8 | 3.5 | 10.4 |
| 0°C | - | 4.6 | 5.8 | 1.9 | 4 | - | 1.5 | 6.2 | 3.9 | 12 |
| -5°C | - | 5.3 | 5.5 | 1.9 | 4 | - | 1.2 | 6.5 | 5 | 11.4 |
| -10°C | - | 5.4 | 6 | 1.8 | 4.3 | - | 1.7 | 7.3 | 4.7 | 12.7 |
| -15°C | - | 6 | 6 | 2.2 | 4.2 | - | 1.2 | 7.8 | 5 | 13 |
| -20°C | - | 5.8 | 6.3 | 2.2 | 4.1 | - | 1.1 | 7 | 5 | 12.6 |
| -25°C | - | 5.4 | 5.1 | 1.6 | 3.7 | - | 1.1 | 7.3 | 4.3 | 11.1 |
| -30°C | - | 5.6 | 5.2 | 1.7 | 3.6 | - | 1.3 | 6.3 | 4.2 | 11.9 |

Values from Claudy et al.1991.

Table 3. Influence of n-Alkane addition on AAG Thermal Behavior

| % n-Alkane | Tg (°C) | DCp (J/g/K) | DHd (J/g)* | DHsl (J/g)** |
|--------------|---------|-------------|------------|--------------|
| 0 (Neat AAG) | -11.4 | 0.337 | - | - |
| 3% C20H42 | -29.2 | 0.134 | 217.5 | 226.7 |
| 3% C24H50 | -20.4 | 0.266 | 222.5 | 230.2 |
| 3% C28H58 | -15 | 0.255 | 252.5 | 245 |
| 3% C32H66 | -13 | 0.295 | 239.8 | 254.6 |
| 3% C36H74 | -10.8 | 0.3 | 245.8 | 256.6 |
| 3% C40H82 | -12.5 | 0.304 | 220.4 | 215.6 |
| 1.66% C24H50 | -15.4 | 0.244 | 118.5 | 230.2 |
| 2.04% C24H50 | -21.3 | 0.158 | 233.3 | 230.2 |
| 3.11% C24H50 | -21.3 | 0.174 | 236.5 | 230.2 |
| 5.35% C24H50 | -18.5 | 0.22 | 238 | 230.2 |

*Dissolution and **Solid-Liquid Transition Enthalpy Variations, respectively.

Fig 1. DSC curves of SHRP Asphalts.

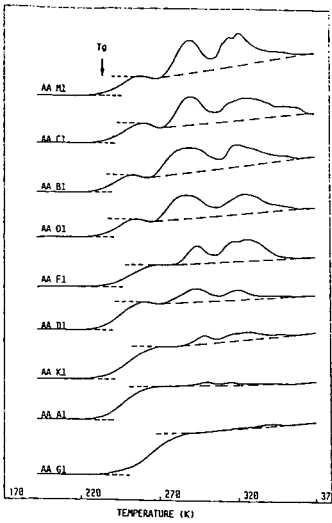


Fig 2. Effect of the Low Temperature Conditioning Time on DSC Curves for AAG and AAM.

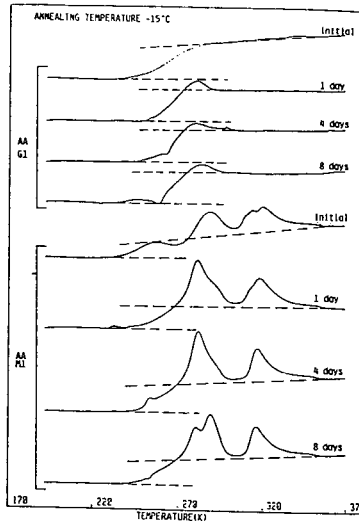


Fig 3. Change in Creep Compliance due to Physical Hardening Asphalt #12

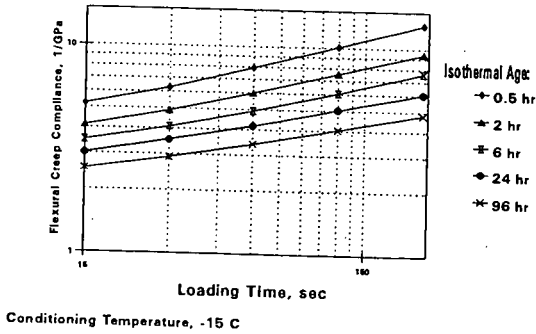
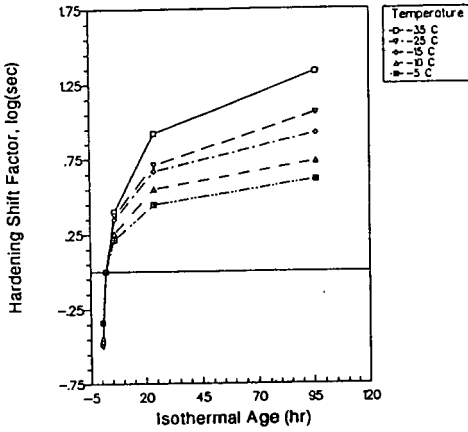


Fig 4. Physical Hardening Trends of Asphalt AAM at Different Temperatures



Reproduced from Anderson et al.1991, with Dr Anderson's permission

Fig 5. Effect of the Conditioning Temperature on DSC Curves for Asphalt AAM.

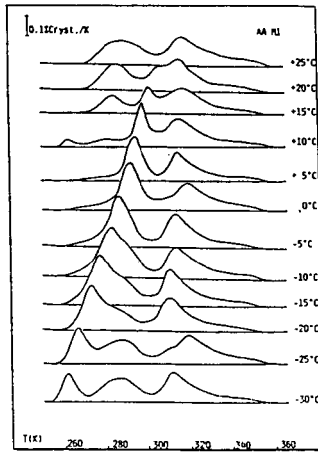
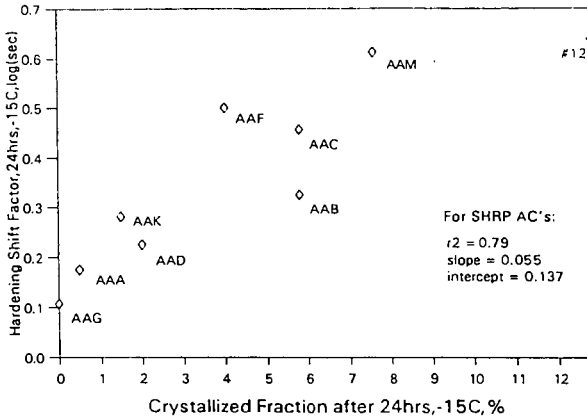
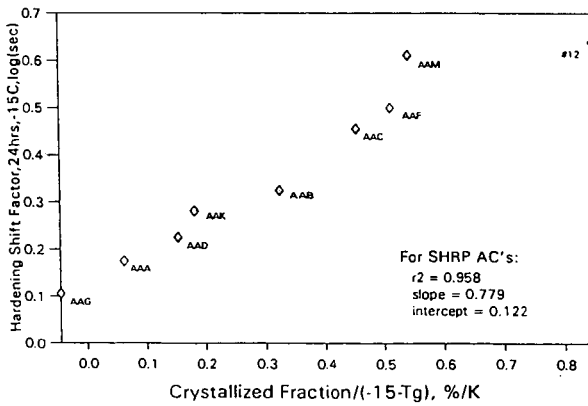


Fig 6. AC Hardening vs Crystallized Fraction



SHRP AC Hardening Shift Factor from Anderson et al. 1991

Fig 7. AC Hardening vs Crystallized Fraction and Tg



Crystallized Fraction & Glass Transition Temperature (Tg) by Differential Scanning Calorimetry (DSC)
 Crystallized Fraction and Glass Transition Temp after 24 hr at -15C
 Hardening Shift Factor from Anderson, et al., 1991

Fig 8. DSC Curves of Pure n-Alkanes.

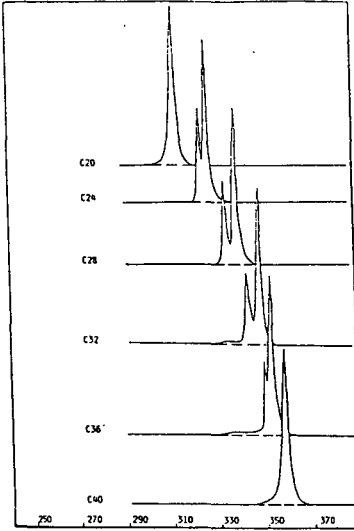


Fig 9. DSC Curves for AAG Doped with n-Alkanes.

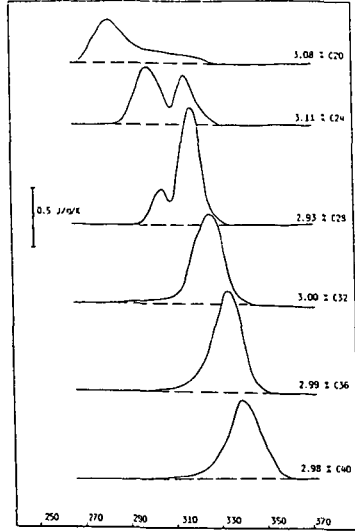


Fig 10. DSC Curves for AAG Doped with n-C24

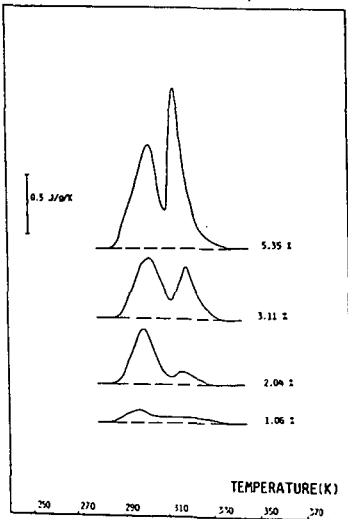


Fig 11. DSC Curves for AAM Doped with n-C24

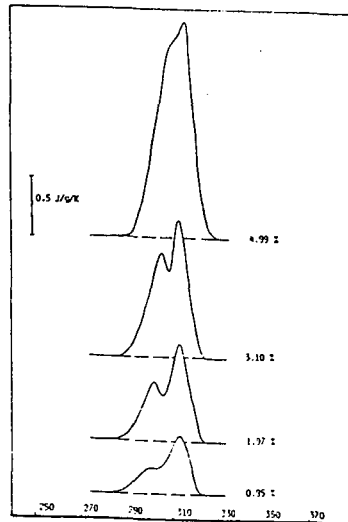


Fig 12. Influence of n-Alkane Addition on Thermomicroscopy Images for Asphalt AAG.

